

Derivation of relativistic SEP properties through neutron monitor data modeling

This content has been downloaded from IOPscience. Please scroll down to see the full text.

2015 J. Phys.: Conf. Ser. 632 012076

(<http://iopscience.iop.org/1742-6596/632/1/012076>)

View [the table of contents for this issue](#), or go to the [journal homepage](#) for more

Download details:

IP Address: 69.163.163.203

This content was downloaded on 26/06/2016 at 15:30

Please note that [terms and conditions apply](#).

Derivation of relativistic SEP properties through neutron monitor data modeling

C Plainaki^{1,2*}, M Laurenza¹, H Mavromichalaki², M Storini¹, M Gerontidou²,
A Kanellakopoulos², M Andriopoulou³, A Belov⁴, E Eroshenko⁴, V Yanke⁴

¹INAF-IAPS, Via del Fosso del Cavaliere, 00133, Rome, Italy

²Nuclear and Particle Physics Section, Physics Dpt., National and Kapodistrian University of Athens, Greece

³Space Research Institute, Austrian Academy of Sciences, Graz, Austria

⁴Institute of Terrestrial Magnetism, Ionosphere and Radio Wave Propagation by Pushkov (IZMIRAN), Moscow, Russia

E-mail: christina.plainaki@iaps.inaf.it

Abstract. The Ground Level Enhancement (GLE) data recorded by the worldwide Neutron Monitor (NM) network are useful resources for space weather modeling during solar extreme events. The derivation of Solar Energetic Particles (SEPs) properties through NM-data modeling is essential for the study of solar-terrestrial physics, providing information that cannot be obtained through the exclusive use of space techniques; an example is the derivation of the higher-energy part of the SEP spectrum. We briefly review how the application of the Neutron Monitor Based Anisotropic GLE Pure Power Law (NMBANGLE PPOLA) model (Plainaki et al. 2010), can provide the characteristics of the relativistic SEP flux, at a selected altitude in the Earth's atmosphere, during a GLE. Technically, the model treats the NM network as an integrated omnidirectional spectrometer and solves the inverse problem of the SEP-GLE coupling. As test cases, we present the results obtained for two different GLEs, namely GLE 60 and GLE 71, occurring at a temporal distance of ~ 11 years.

1. Introduction

Ground-level enhancement (GLE) events are related to the most energetic class of solar energetic particle (SEP) events, associated with solar flares and/or coronal mass ejections (CMEs), and requiring acceleration processes that produce particles with energies ≥ 500 MeV upon entry in the Earth's atmosphere. This class of SEPs can produce showers of secondary particles with sufficient energy to be detected by ground-level Neutron Monitors (NMs) and with intensities that exceed the Galactic Cosmic Ray (GCR) background (see, among others, [1]).

Several techniques for modeling the dynamical behavior of GLEs are presently available (e.g. [2 - 11]). Typically, the responses of ground level NMs to SEPs are modeled to determine both the best-fit spectrum and the flux spatial distribution of the solar particles during a GLE event. Usually, a least squares procedure is applied in order to define the values of the parameters that best fit the GLE model in use. The functions considered to perform the fit represent the physical processes involved in the

* Corresponding author



particle rigidity distribution and propagation as well as the atmospheric response to the incoming particle fluxes. One of the most intriguing open questions, to which GLE modeling can give important insights, is the determination of the acceleration mechanism that is responsible for the production of relativistic SEPs. Whereas numerous techniques, based on the analysis of satellite data, have been successfully applied in order to get insights into which acceleration mechanism is the responsible one for a specific event (i.e. acceleration at the flare reconnection sites or acceleration at the shocks driven by CMEs propagating through the solar corona and in the interplanetary space), the incorporation of ground-based methods can integrate these analyses by providing information also on the high-energy component of the SEP population. In order to determine the direction of arrival of the solar particles at the Earth during a GLE, models can assume either a pitch-angle distribution function (see [12 - 13]) or, simply, a latitude and longitude-dependent function (that represents the spatial diffusion of the solar particles around the apparent source direction), without inserting directly the interplanetary magnetic field (IMF) direction information in the model (see [4-5], [7], [10-11], [14]). Whereas the alignment of the solar particle velocity with the IMF could be an indication of propagation along the magnetic field lines almost without scattering ([12]), [15] argued that there is no reason why the magnetic field measured by a satellite at some point would be the same as the average field sampled by the particles over their orbit. Such was the case of GLE 59 (on 2000 July, 14), when the derived asymptotic latitude of the anisotropy in the Geocentric Solar Ecliptic (GSE) coordinate system deviated from the IMF latitude up to almost 100° (opposite hemisphere) during the event maximum [15]. In this view, it can be generally stated that the model-assumption of particle propagation around the local IMF vector is not always a quantity to be inserted a priori as a pre-defined input while modeling GLEs.

Current modeling techniques incorporate realistic geomagnetic field models (e.g.: Tsyganenko, 1989 – T89; 1996 – T96) which take into account possible geomagnetic disturbances; the choice of the magnetic field model to be incorporated inside a GLE model has a major weight in the determination of the actual SEP parameters. Indeed, [16] showed that the use of different magnetic field models (T89 and T96) inside the NMBANGLE PPOLA model, influence the derived results to an extent depending on the SEP energy. For the case of GLE 71, [16] found that the modeled solar proton spatial distribution (for rigidities of ~ 1 GV) is less diffused around the apparent source direction when the T96 (rather than the T89) model is considered. In particular, the angular distribution around the apparent source has a width equal to 19° and 32° when T96 and T89 are considered, respectively. For the 2 GV particles, both models gave similar results. The accurate modeling of a GLE event depends also on two other important factors: the number of the NMs used in the analysis and their spatial distribution around the world; for example, in order to avoid a biasing of the modeling-results, it is important to use data originating from NMs that are almost equally distributed between the two hemispheres (see also [17]).

In this work we perform a brief comparative examination of the results obtained from the NMBANGLE PPOLA model application to GLE 60 (on 2001 April, 15) and GLE 71 (on 2012 May, 17) that took place at a temporal distance of ~ 11 years, both occurring in the maximum solar activity phase, although the sunspot number in 2012 was significantly lower than its value in 2001. The modeling results presented here are based exclusively on the use of ground-based NM data hence our technique is completely independent from the satellite measurements analysis. Consequently, an a posteriori comparison of model-derived quantities with those obtained from the satellite measurements (e.g. GOES energetic particle data) can be used to validate the model itself. The scope of this comparative study is to show that GLE modeling based exclusively on the use of NM-data, can provide: a) the SEP spectrum reconstruction, b) an explanation of the form of the GLE time-intensity profiles on the basis of the solar particle arrival directions and the NM asymptotic directions of viewing, and c) quantitative information on the SEP flux evolution and direction upon arrival in the Earth's atmosphere. In Section 2, we provide a brief description of the NMBANGLE PPOLA modeling technique and a short summary of two GLEs under study. In Section 3 we perform a

comparative analysis of the obtained results and finally, in Section 4, we give the main conclusions of the current study.

2. Modeling technique and events description

2.1. The NMBANGLE PPOLA model

The NMBANGLE PPOLA model is a modified version of the original NMBANGLE model [7], which is based on the coupling coefficient method [18] applied numerous times in the past (e.g., [4-5], [7], [14]). The NMBANGLE PPOLA model couples SEPs (primary particles) at a selected altitude in the Earth's atmosphere with the secondary ones detected by ground-level NMs during GLEs. This model dynamically calculates the SEP spectrum and the SEP flux spatial distribution at some altitude in the atmosphere. A power-law SEP spectrum with two free parameters (spectral index and amplitude) is assumed. SEPs are assumed to be protons in the model's current version. The details of the physics considered in the NMBANGLE and the NMBANGLE PPOLA models have been provided in the past (see [7], [10-11]). In this Section we only give a very brief description of the model.

The NMBANGLE PPOLA model uses as inputs the response of the worldwide NM network to the high-energy solar protons (i.e., ≥ 500 MeV) and the disturbance level of the geomagnetic field (through the use of the k_p index). The NM network is treated as an integrated omnidirectional spectrometer able to measure the characteristics of the relativistic primary flux at a selected altitude ($h_0=20$ km) in the Earth's atmosphere. GLE data from NM stations widely distributed around the world are incorporated (for a detailed description of the format of the GLE data used in the model, see [10]). In this context, the modeling of the NM response to an anisotropic SEP flux and the solving of the inverse problem can provide the actual characteristics of the relativistic SEPs that are responsible for the event. The results of the application of both NMBANGLE and NMBANGLE PPOLA models to past GLEs have been, in general, in good agreement with space observations, when available ([7], [10-11]). We note that due to the particle motion inside the geomagnetic field, each ground level detector is capable of recording secondary particles produced by primaries arriving from a set of directions in space, depending on their energy, known as the station's asymptotic directions of viewing. For the evaluation of the NM directions of viewing, the method described by [19] is applied; the assumption that the Earth's magnetospheric field can be adequately described by the T89 model ([20]) is considered. In the particle trajectory calculation, the relativistic SEPs have been considered to have a vertical incidence at each neutron monitor location.

According to the NMBANGLE PPOLA model, the possible time variations, $\Delta N/N_0$, of the total neutron counting rate, N_0 , observed at cut-off rigidity R_c , geographic latitude ϕ and longitude λ , at level h in the atmosphere and at some moment t , are determined by the following expression ([7], [10]):

$$\frac{\Delta N(R_c, h, t, t_0)}{N_0(R_c, h, t_0)} = \int_{R_c}^{R_u} \frac{W(R, h, t_0) \cdot \Delta I(R, \Omega(R, t), t)}{I_0(R, t_0)} dR = \int_{R_c}^{R_u} \frac{W(R, h, t_0) \cdot A(R, \Omega(R, t), t) b(t) R^{\gamma(t)}}{I_0(R, t_0)} dR \quad (1)$$

where $W(R, h, t_0)$ is the rigidity-dependent coupling function (properly normalized to have values in the 0-1 range) between secondary and primary particles arriving at altitude h_0 (with $h_0 > h$) in the Earth's atmosphere (see [7] for analytical expression); $\Delta I(R, \Omega(R, t), t) = I(R, \Omega(R, t), t) - I_0(R, t_0)$ is the increase of the primary flux due to the arrival of SEPs at altitude h_0 , assumed to follow a power law in rigidity ([7]), i.e. $\Delta I(R, \Omega(R, t), t) = A(R, \Omega(R, t), t) \cdot b(t) R^{\gamma(t)}$; $\gamma(t)$ is the exponent of the power-law SEP spectrum; $A(R, \Omega, t)$ is a dimensionless normalized function that describes the spatially anisotropic SEP arrival at altitude h_0 , with $\Omega(R, t)$ being the angle defined by the direction of viewing for vertical incidence at a NM for a rigidity R and the vertical direction of the apparent SEP source at altitude h_0 , as defined in [7]; R_u is the theoretical upper limit for the rigidity of the SEP particles, a parameter that in the model is specified a priori (here 8 GV) without a big loss in the estimation accuracy of the other parameters ([4]); $b(t)$ is the amplitude of the SEP differential flux (in

protons $\text{m}^{-2} \text{s}^{-1} \text{sr}^{-1} \text{GV}^{-1}$); and $I_0(R, t_0)$ is the GCR differential flux (in protons $\text{m}^{-2} \text{s}^{-1} \text{sr}^{-1} \text{GV}^{-1}$). In our model, we define $A(R, \Omega(R, t), t)$ as in [7]:

$$A(R, \Omega, t) = \exp\left(-n_a(t)^2 \sin^2 \frac{\Omega(R, t)}{2}\right) \quad (2)$$

where $n_a(t)$ is a dimensionless parameter that characterizes the width of a primary solar particle beam, arriving at altitude h_o , around a specific location, whose latitude and longitude are free parameters for the model. Through the selection of the mathematical form described in Equation (2), the NMBANGLE PPOLA model parameterizes the level of the primary particle flux anisotropy by the use of variable $n_a(t)$, which is dynamically determined after each model run. Big values for $n_a(t)$ mean that the arriving SEP flux is narrowly distributed around a specific location at altitude h_o , whereas smaller values for $n_a(t)$ mean that the SEP flux is more widely distributed in longitudes and latitudes. This parameter is determined independently from the magnitude of the primary SEP intensity. However, it is the product of the anisotropy function with the primary spectrum that gives the total behaviour of the primary flux responsible for the event registered at ground level. A least-square fitting technique based on the Levenberg Marquardt algorithm allows an efficient derivation of the optimal solution for each time interval and the determination of the GLE parameters evolution. Five-minute GLE data from NM stations of the worldwide network are incorporated to fit Equation (1). Each time represents the start of a five minute integrated time interval.

2.2. Description of GLE 60, GLE 71 and related SEP events

On 2001 April 15, a strong flare (X14.4/2B) was observed at the west limb of the solar surface at the position S20W85, associated with a fast CME ($>1200 \text{ km/s}$) (see [21], [22] for details). Following the detection of gamma and X-rays, the High Energy Proton and Alpha Detector on board GOES 10 satellite recorded sudden increases in relativistic protons (510-700 MeV) between 13:50 UT and 13:55 UT [6]. High energy protons and possibly neutrons, associated with the above mentioned solar events, were detected by the ground-level NMs of the worldwide network, starting at about 13:50 UT, in 5-min NM data (see Fig. 1). The event was seen by polar and mid-latitude NMs, as well as by some low-latitude NMs (see [10] for a full description). The maximum NM % count increase was 225.4%, at South Pole NM.

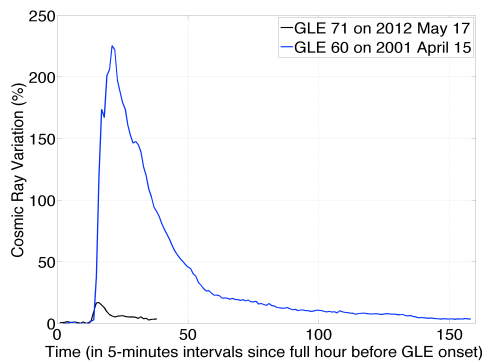


Figure 1: Relative counting rate variation of the South Pole neutron monitor during GLE 60 (in blue) and GLE 71 (in black). The x-axis unit is 5-minutes intervals since the full hour before GLE onset.

at South Pole NM. Among the numerous mid-latitude NMs, GLE71 was registered at Kiel, at Kerguelen and at Yakutsk. The low-latitude NMs (high magnetic cut-off rigidity, R_c) did not register GLE 71 (e.g., [24]). Figure 1 illustrates the percentage variation of the counting rate registered at the NM of South Pole during these two events as a function of time (measured in 5-minutes intervals since full hour before GLE onset). The pre-increase baseline period used to derive the percentage is 301.622 counts/s for GLE71 (at 0:00 – 01:00 UT) and 243.361 counts/s for GLE60 (at 12:00 - 13:00 UT).

3. Brief comparative analysis - Discussion

3.1 SEP spectrum

The modeled SEP rigidity spectra are computed for both GLEs, every 5 minutes during their evolution. In Fig. 2, we present the SEP rigidity spectra derived by the application of the

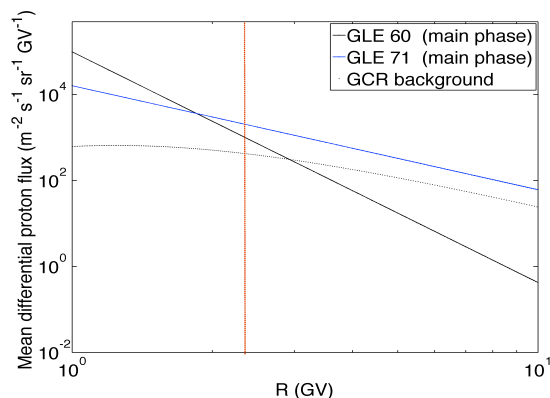


Figure 2: GLE 60 and GLE 71 spectra at the main phases of each event, obtained from the application of the NMBANGLE PPOLA model. The red line marks the 3 GV rigidity value over which the GLE71 spectrum is less reliable. Dot line represents the GCR background computed through the CRÈME model (<https://creme.isde.vanderbilt.edu/>) for May 17, 2012.

is about one order of magnitude higher. Moreover, for GLE71, the predicted proton spectrum continues to exceed the GCR background (dotted line in Figure 3) even at rigidities > 3 GV (red line). At 3 GV our modeled intensities are almost one order of magnitude higher than those shown in [12] and [9]. Perhaps the anisotropic direction of arrival of solar particles might play a role in the high intensities estimated by our model. In a detailed study of GLE 71 using the NMBANGLE PPOLA tool, [11] estimated the expected anisotropy in the arrival direction, through the calculation of the parameter n_a (see Section 2.1), which was found to take a non zero value in the time interval 2012 May 17 02:15-02:20 UT. It is underlined that this parameter expresses exactly the spread of the primary flux over latitudes and longitudes (for a complete explanation of the n_a meaning see [7]). Therefore the high rigidity particles (if present) could be sensed through their secondaries only by those NMs that had direction of viewing (corresponding to these high rigidities, i.e. in the range 3-10 GV) located close to the maximum flux of the apparent particle source. The small magnitude of this event in any case can be an additional reason for which the increases in the NMs were not significant and the latitude effect was absent. The latter has been pointed out also by other researchers as well (see Section 4.3 in [25]). A further analysis regarding these issues is, in any case, necessary and intended in the near future.

According to Fig. 2, the NMBANGLE PPOLA model application gives a harder spatially averaged spectrum for GLE 71 than for GLE 60: in the rigidity range from 2 to ~ 4 GV the mean differential flux of the primary SEPs during GLE 71 is higher than its values during GLE 60, by up to one order of magnitude. This result seems to contradict the fact that during GLE 60, SEPs with higher maximum energy than those during GLE 71 have been observed [11]. However, this result can be explained on the basis of the following arguments. The above comparison of the two SEP spectra refers to the main phase of each event, i.e. after the registration of the maximum NM intensity variation, and not to the main SEP acceleration phase that had taken place during the first 5-min intervals after the flare in each case. The high rigidity SEPs during GLE 60 were registered mainly during this initial phase (see for example [10]). Therefore a relatively soft SEP spectrum in the main phase of GLE 60 is reasonable. Moreover, although the GLE 60 shows intensity variations in the

ground observations significantly higher than during GLE 71, the spatial distribution of the primary flux is more anisotropic, consistently with NM observations [10]. As a consequence, the peak secondary flux (at the ground) can be measured mainly at specific locations that are magnetically favorable with respect to the SEP source. Therefore, the spatially averaged modeled-SEP spectrum in Fig. 2 is less representative of the actual GLE 60 event evolution, since the averaged SEP fluxes smoothen too much the actual flux variations in rigidity. At this point we would like to emphasize that an averaging of the differential primary flux over all longitudes and latitudes is necessary in order to obtain the mean SEP spectrum per solid angle unit; such a quantity can be easily compared with the one obtained from the omnidirectional measurements of different kind or from other models. Finally, GLE 60 took place inside a Forbush Decrease (that was indeed modeled in NMBANGLE PPOLA [10]) where the GCR intensity (I_0 in Eq. 1) was lower than the one during GLE 71, that took place in a relatively quiet period. This might have affected the computation of the modeled spectra.

In the low rigidity range (≤ 2 GV), the mean differential flux of the SEPs during GLE 60 is bigger than its values during GLE 71, by up to one order of magnitude. This result is in good agreement with the NM observations that are higher during GLE 60 (by more than one order of magnitude at the South Pole NM) than during GLE 71. We note that in the case of GLE 60, in the lower rigidity range (i.e. < 2 GV), the NMBANGLE PPOLA spectrum is in good agreement with the spectrum calculated by other models (e.g. [6]). On the other hand, in the higher rigidity range, the estimated NMBANGLE PPOLA intensities seem to be overestimated: for GLE 60 they are in general higher than those estimated by [6], where a modified power law spectrum was assumed. Nevertheless, spacecraft measurements at rigidities ≥ 1 GV are not always available (e.g. for GLE 60) and modeling the ground based-data remains an important tool for the derivation of the SEP characteristics at 1 AU, integrating also the information obtained by satellite instruments that cover the lower rigidity range (e.g. proton detectors onboard GOES). Since NMs are distributed in different geographical latitudes and longitudes, they provide information related to a different part of the SEP spectrum. Therefore, NM-data from a network of stations distributed geographically in the most possible balanced way is necessary for analyses of this kind.

3.2 SEP fluxes

Comparison of the extrapolated model-derived flux of lower-energy (> 100 MeV) SEPs with 5-min GOES observations, for both GLE 60 and GLE 71 events, has shown that in general the NMBANGLE PPOLA model simulates adequately the real SEP flux in the main event-phase. For example, in the case of GLE 71, for the time period after 02:00 UT, the > 100 MeV modeled and GOES fluxes differ by a factor lower than ~ 3 (see Fig. 6 in [11]). Similarly, in the case of GLE 60, for the time period after 14:00 UT, the > 100 MeV modeled and GOES fluxes differ by a factor lower than ~ 4 (see Fig. 9 in [10]). On the other hand, in the initial time period of each event the model based on neutron monitor data gives in general higher SEP fluxes than the ones observed by satellite detectors, mainly at low rigidities. To explain this difference, one should consider the streaming limit effect, which currently has not been integrated in the NMBANGLE PPOLA model. During a SEP event, the intensity of the MeV-energy particle fluxes can exhibit a plateau of about $100 \text{ cm}^{-2} \text{ s}^{-1} \text{ MeV}^{-1}$, varying by a factor of two among different events [27]. This phenomenon, known as the ‘streaming limit’ [27], can result in suppressing the low-energy particle arrival below the levels expected from higher-energy spectral responses. It would be very useful, therefore, if during future GLE modeling efforts the streaming effect were taken into account while extrapolating the model-derived data to the lower energy ranges.

3.3 SEP anisotropy direction

The direction of the apparent source of solar particles at a selected altitude in the Earth's atmosphere, a quantity that is generally difficult to determine, is a dynamical output of the NMBANGLE PPOLA model. The time-dependent variation of the position of this apparent source can explain the differences in the profiles of NMs with similar cut-off rigidities, located in different places though. In case of GLE 71, in the initial event phase, the apparent SEP source direction was located in

the Northern hemisphere, whereas with time, it moved to lower latitudes. This result is consistent with the ground-based observations [11]. In case of GLE 60, during the initial phases of the event, the latitude of the apparent SEP source, as obtained by the NMBANGLE PPOLA model, varies significantly around the ecliptic plane. However, in that period, the model results contain large uncertainties due to the extremely anisotropic direction of propagation of the solar particles and due to the big differences in the counting rates recorded between different NMs. In later phases of the GLE 60 event, the apparent source moves northwards. An important reason that most models fail during the rising phase of a GLE is that the SEP flux changes are too dynamic and the models would need data of sufficient statistical accuracy, with sampling times as short as a minute. These data are not always available, since many NM stations have registration systems with larger sampling times. Moreover, it often happens that there is very poor representation of southern viewing directions (see for example [10]). This can significantly bias the modeling results, especially those considering the position of the anisotropy source, which seems to be the less reliably modeled parameter in the NMBANGLE PPOLA model.

4. Conclusions

The SEP spectra during GLE 60 and GLE 71 as well as their spatial distribution have been estimated through modeling of the ground-based NM data. The main results can be summarized as follows.

- A hard rigidity spectrum of accelerated protons was found during the initial phase of GLE 60 and a rather soft spectrum in later phases, i.e. after 14:00 UT ($\gamma \sim -5.5$).
- During the main phase of GLE 71, the rigidity spectrum index γ was estimated to be ~ -2.1 ; in later phases, i.e. after 02:20 UT, a softer spectrum of accelerated protons ($\gamma \sim -3.8$) has been derived. The corresponding values for the energy spectrum are -1.55 and -2.4, respectively (see [11]).
- The results for GLE 71 are consistent with the typical range found by [28] for shock wave acceleration in case of relativistic SEP events (see also [29]), although a direct flare contribution cannot be excluded (see also [11]).
- The model-results can provide realistic estimation of the SEP fluxes in the energy range where NM increases are registered.
- For both GLEs, the model seems to overestimate the spatially averaged SEP spectrum in the high rigidity range, where no NM increases are registered.
- Comparison of the results obtained for the two events is valid mainly in the rigidity range 1-3 GV. The spectrum computed in the event main phase results to be harder for GLE 71. This could be due to the different SEP flux spatial distribution with respect to the NM direction of viewing and the different GCR background level (that is reduced during GLE60);
- The integral SEP fluxes calculated by the NMBANGLE PPOLA model are in good agreement with GOES observations if extrapolated to the lower energy range.

The NMBANGLE PPOLA results will be more reliable during future model-applications to GLEs, if the NM data-quality is high hence the NM data used in the model should be provided with the same quality standards. The NMBANGLE PPOLA results can be also used for radiation dose calculations (as in [17]) in the context of space weather perspectives. In our model, the position of the GLE source outside the atmosphere has been considered to be the most significant factor determining the propagation and final registration of the secondaries at ground level. Up to now, this assumption has been considered also in other modeling efforts for different GLEs (see [6], [8], [12]). However, other phenomena, like the diffusion of the secondary particles inside the atmosphere could also have a role in the interpretation of the ground-level intensity time profiles during a GLE and should be taken in detail into account during future analysis.

Acknowledgements

The authors acknowledge all colleagues at the NM stations who kindly provided us with the data used in this study and the Referees for useful comments. Thanks are also due to the High-resolution Neutron Monitor NMDB database, founded under the European Union's FP7 Program (contract No. 213007) for providing cosmic ray data.

References

- [1] Lopate C 2006 In: Gopalswamy, N, Mewaldt, R, Torsti, J (eds) *Solar Eruptions and Energetic Particles*, Geophysical Monograph Series **165**, AGU Press, Washington 283
- [2] Shea M A and Smart D F 1982 *Space Sci. Rev.* **32** 251
- [3] Humble J E, Duldig M L, Smart D F and Shea M A 1991 *Geophys. Res. Lett.* **18** 737.
- [4] Belov A, Eroshenko E, Mavromichalaki H, Plainaki, C and Yanke V 2005, *Ann. Geophys.* **23** 2281
- [5] Belov A V, Eroshenko E A, Mavromichalaki H, Plainaki C and Yanke VG 2005 *Proc. 29th Inter. Cosmic Ray Conf.* vol 1, p 189.
- [6] Bombardieri D J, Michael K J, Duldig M L and Humble J E 2007 *Astrophys. J.* **665** 813
- [7] Plainaki C, Belov A, Eroshenko E, Mavromichalaki H and Yanke V 2007 *J. Geophys. Res. A* **112** 4102
- [8] Vashenyuk E V, Balabin Y V and Gvozdevsky B B 2011 *ASTRA* **7** 459
- [9] Mishev A L, Kocharov L G and Usoskin I G 2014 *J. Geophys. Res.* **119** 670
- [10] Plainaki C, Mavromichalaki H, Belov A, Eroshenko E, Andriopoulou M and Yanke V 2010 *Sol. Physics* **264** 239
- [11] Plainaki C, Mavromichalaki H, Laurenza M, Gerontidou M, Kanellakopoulos A and Storini M 2014 *Astrophys. J.* **785** 160
- [12] Balabin, Y V, Germanenko A V, Gvozdevsky B B and Vashenyuk E V 2013 *J. of Physics: Conference Series* **409** 012053
- [13] Bütikofer R, Flückiger E O, Desorgher L, Moser M R and Pirard B 2009 *Adv. Space Res.* **43** 499
- [14] Plainaki C, Mavromichalaki H, Belov A, Eroshenko E and Yanke V 2009 *Adv. Space Res.* **43** 474
- [15] Bieber J W, Droge W, Evenson P A, Pyle R, Ruffolo D, Pinsook U, Tooprakai P, Rujiwarodom M, Khumlumlert T and Krucker S 2002 *Astrophys. J.* **567** 622
- [16] Kanellakopoulos A, Plainaki C, Mavromichalaki H, Laurenza M, Gerontidou M, Storini M and Andriopoulou M 2014 *EGU General Assembly 2014* **16**, EGU2014-461
- [17] Bütikofer R and Flückiger E O 2013 *J. of Physics: Conference Series* **409** 012166
- [18] Dorman LI 2004 *Astrophys. Space Sci. Libr.* **303**
- [19] Plainaki C, Mavromichalaki H, Belov A, Eroshenko E and Yanke V 2009 *Adv. Space Res.* **43** 518
- [20] Tsyganenko N A 1989 *Planet. Space Sci.* **37** 5
- [21] Muraki Y, Matsubara Y, Masuda S, Sakakibara S, Sako T, Watanabe K, Bütikofer R, Flückiger E O, Chilingarian A, Hovsepyan G, Kakimoto F, Terasawa T, Tsunesada Y, Tokuno H, Velarde A, Evenson P, Poirier J and Sakai T 2008 *Astropart. Phys.* **29** 229
- [22] Gopalswamy N, Lara A, Yashiro S and Howard R A 2003 *Astrophys. J. Lett.* **598** 63
- [23] The IceCube Collaboration 2013 *Science* **342** 6161
- [24] Signoretto F & Storini M 2013 *INAF Report IAPS-2013-05* (Rome, Italy: Institute for Space Astrophysics and Planetology)
- [25] Li, C, Firoz, K A, Sun, L P, and Miroshnichenko, L I. 2013 *Astrophys. Journal* **770** 34
- [26] Lovell J L, Duldig M L, Humble J E 1998 *J. Geophys. Res.* **103** 23733
- [27] Reames D V and Ng C K 1998 *Astrophys. J.* **504** 1002
- [28] Ellison D C and Ramaty R 1985 *Astrophys. Journal* **298** 400
- [29] Mewaldt R A et al 2012 *Space Sci. Rev.* **171** 97